frontiers | Frontiers in Agronomy

TYPE Original Research
PUBLISHED 04 February 2026
DOI 10.3389/fagro.2026.1748798

OPEN ACCESS

EDITED BY
Mario Licata,
University of Palermo, Italy

REVIEWED BY
Leo Sabatino,
University of Palermo, Italy
Domenico Ronga,
University of Salerno, Italy

*CORRESPONDENCE
Leonardo Verdi
leonardo.verdi@unifi.it

RECEIVED 18 November 2025
REVISED 07 January 2026
ACCEPTED 12 January 2026
PUBLISHED 04 February 2026
CORRECTED 27 March 2026

CITATION
Barrera W Jr., Morbidini F, Maucieri C, Giordano M, Pogačar T, Flajšman M, Ghinassi G, Verdi L, Ferrise R and Dalla Marta A (2026) Quantifying consumptive water footprints of soybean in rainfed and irrigated systems under climate change scenarios. *Front. Agron.* 8:1748798. doi: 10.3389/fagro.2026.1748798

Quantifying consumptive water footprints of soybean in rainfed and irrigated systems under climate change scenarios

Wilfredo Barrera Jr.[1,2,3], Francesco Morbidini[4], Carmelo Maucieri[4], Maria Giordano[4], Tjaša Pogačar[5], Marko Flajšman[5], Graziano Ghinassi[1], Leonardo Verdi[1]*, Roberto Ferrise[1] and Anna Dalla Marta[1]

[1]Department of Agriculture, Food, Environment and Forestry (DAGRI), University of Florence, Florence, Italy, [2]Department of Science, Technology, and Society, University School for Advanced Studies IUSS Pavia, Pavia, Italy, [3]Mathematics and Natural Sciences Department, College of Arts and Sciences, Southern Luzon State University, Lucban, Quezon, Philippines, [4]Department of Agronomy, Food, Natural resources, Animals and Environment (DAFNAE), University of Padua, Padua, Italy, [5]Department of Agronomy, Biotechnical Faculty, University of Ljubljana, Ljubljana, Slovenia

Introduction: Understanding climate change impacts on water footprints (WFs) is crucial for sustainable soybean production.

Methods: We utilized previously calibrated AquaCrop model to assess baseline (1981–2010) and future climate change impacts on soybean WFs under Shared Socio-economic Pathways (SSPs) emission scenarios (SSP1-2.6, SSP2-4.5, and SSP5-8.5) in rainfed and irrigated systems.

Results: The $WF_{rainfed}$ varied across locations in the baseline period, with Cesa having the highest values and Ljubljana the lowest. Blue WF and $WF_{irrigated}$ increased as the readily available water (RAW) depletion threshold for irrigation decreased, with no significant differences in $WF_{irrigated}$ across irrigation strategies. Future climate change showed varying effects on $WF_{rainfed}$ and $WF_{irrigated}$. Under SSP1-2.6 and SSP5- 8.5, $WF_{rainfed}$ is projected to increase from mid (2061–2080) to far future (2081– 2100). Whereas, a decrease is projected from near (2041–2060) to far future under SSP2-4.5. $WF_{irrigated}$ is expected to decrease in Castelfranco and Cesa but to increase in Ljubljana. Under SSP5-8.5, $WF_{irrigated}$ increased from near to far future. Whereas, SSP2-4.5 showed a decline, except in Ljubljana from near to mid-future. Under SSP1-2.6, $WF_{irrigated}$ decreased from near to mid-future but increased from mid to far future. Blue WF followed similar patterns to these projections. Irrigation strategies have minimal effects on consumptive WFs but significantly influence blue water use and yield.

Discussion: Future climate change will differentially impact rainfed and irrigated soybean WFs, emphasizing the need for targeted irrigation water management strategies. The findings are essential to making informed decisions for sustainable soybean production in the study areas.

KEYWORDS

AquaCrop model, blue water, crop water requirements, *Glycine max* L., green water, irrigation water management, readily available water

10.3389/fagro.2026.1748798

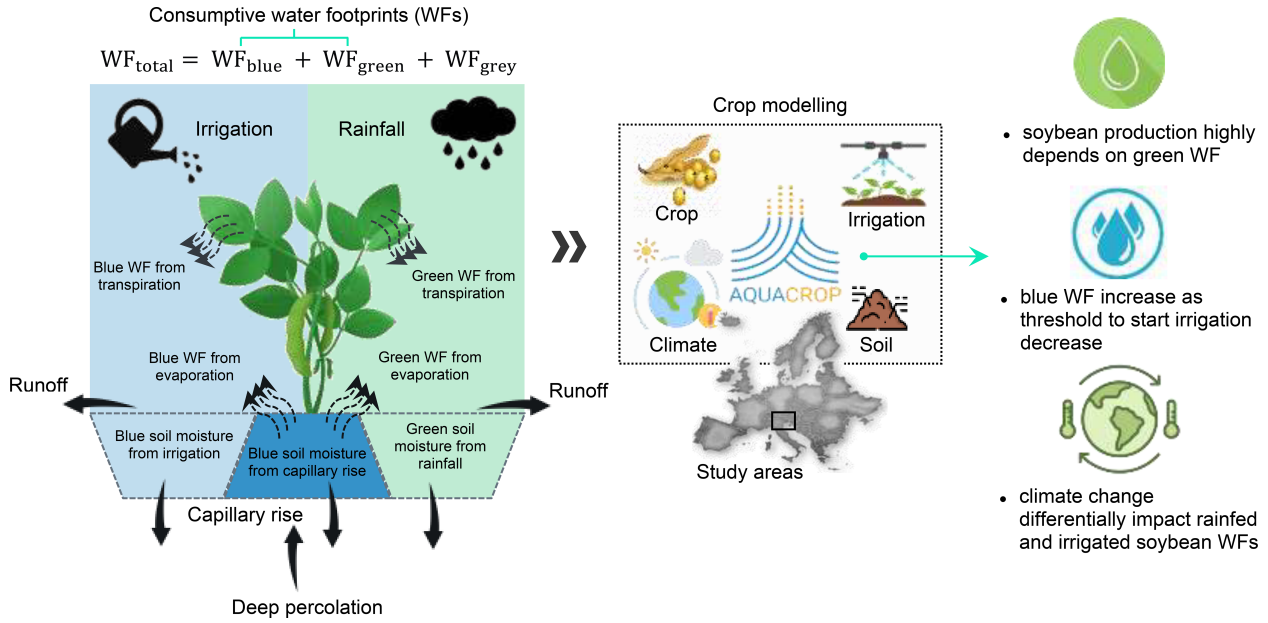

Highlights

- Soybean production across locations highly depends on green water footprint (WF).
- Soybean total WF vary across locations: is highest in Cesa and lowest in Ljubljana.
- Decline in green water, increase in blue water and WF is projected under SSP5-8.5.
- Blue WF and $WF_{irrigated}$ increase as threshold for irrigation decreases.
- Trade-offs between yield and blue WF must be considered when irrigating soybean.

1 Introduction

The concept of a water footprint (WF) provides a novel approach in understanding the relationship between physical and virtual water in agricultural production. Virtual water refers to the amount of water embedded in the production of goods and services. With the increasing intensity of water scarcity brought about by climate change and increasing crop production demand, WF assessment is gaining more importance. Assessment of the WF allows for an understanding of crop water demand and provides recommendations for the proper allocation of agricultural water and the development of water-saving management practices (Gao et al., 2023).

In crop production, the total water footprint (WF_{total}) refers to the type and amount of water resources used to produce primary agricultural products in a certain area. It represents the volumetric measure of freshwater usage for cultivating a crop which can be distinguished into blue, green, and grey water components, respectively (Equation 1) (Chapagain et al., 2006; Mekonnen and Hoekstra, 2014; Shang et al., 2021; Xu et al., 2015).

$$WF_{total} = WF_{blue} + WF_{green} + WF_{grey} \quad (1)$$

The blue water footprint (WF_{blue}) represents the volume of irrigation water that is either evaporated, transpired by crop, or incorporated into plant biomass. Instead, the green water footprint (WF_{green}) is the volume of precipitation stored in the soil that is used by the crop through evapotranspiration. It represents the portion of precipitation that is neither lost as runoff nor contributes to groundwater recharge, but is instead utilized by the crop for growth and lost through soil evaporation (Chukalla et al., 2015; Falkenmark and Rockström, 2006; Hoekstra et al., 2011; Xu et al., 2015). WF_{blue} and WF_{green} are collectively known as consumptive WFs and their reduction in crop production is one of the means of increasing water productivity and reducing water scarcity (Hoekstra, 2017). The WF_{blue} and WF_{green} (m^3 ton^{-1}) of a crop are calculated by dividing the blue ($ET_{c\text{-}blue}$) and green ($ET_{c\text{-}green}$) evapotranspiration over the growing period by the marketable yield, respectively (Chukalla et al., 2015; Mekonnen and Hoekstra, 2011). On the other hand, the grey water footprint (WF_{grey}) refers to the volume of water required to dilute pollutants to agreed maximum acceptable levels (Hoekstra and Chapagain, 2007). In many studies, the WF_{grey} is usually ignored due to the lack of information and the complex nature of pollutants (Xu et al., 2015).

The concept of a WF was introduced by Hoekstra and Hung (2002). Since then, many studies have been conducted to quantify the WF of different agricultural commodities. Most of the studies focused on the spatio-temporal dynamics of green, blue, and grey WFs of different crop species, including cereals, vegetables, fruit crops, oil crops, and fiber

crops. However, the quantification of inter-annual variability and the long-term changes and impacts of climate change on the WF of different crops, with a higher spatial resolution at a macroscopic scale, remains limited (Li et al., 2022; Zhuo et al., 2016a). Most previous studies focused largely on impacts of water use in the production location, particularly in water-stressed areas (Flach et al., 2020).

Crop simulation models (CSMs) are important tools in WF assessment. One example of a CSM is AquaCrop, which is a process-based model that can be used to estimate the WF of crop production under different management practices and climate change scenarios. AquaCrop can also be used to differentiate blue and green water contributions and their respective impacts on crop yield. The performance of this model has proven excellent in understanding the effects of water management practices on blue and green evapotranspiration, yield, and blue and green WFs of various crops. Moreover, the efficacy of the model for the various crops has been demonstrated under diverse conditions and crop production systems, as well as in past and future climate scenarios (Chukalla et al., 2015; Jiang et al., 2022; Yeşilköy and Şaylan, 2020). However, its application to soybean WF assessment on a local scale in Europe to establish baseline information has been relatively scarce. This is attributable to the fact that most studies have been conducted in major soybean-producing countries like Brazil (Ayala et al., 2016; Santos and Naval, 2020, 2022), Argentina (Rodriguez et al., 2021, 2024) and China (Li et al., 2022; Shang et al., 2021; Zhuo et al., 2016a, b, c). While global or regional WF assessments offer broader geographical coverage and generalized results, understanding crop WFs on a local scale is essential for developing precise and effective adaptation strategies in response to climate change (Arunrat et al., 2022).

Soybean is one of the crops of global importance both for humans and animals (Flajšman et al., 2019). In Europe, soybean plays an important role in addressing the deficit in high-protein feed materials (Hiel et al., 2018). The strong reliance of the European Union (EU) on global soybean imports (about 12.4 million tons annually) prompted the European Commission (EC) to implement a plant protein strategy aimed at diminishing the reliance on protein imports from third countries. One objective of this strategy is to enhance the profitability and competitiveness of soybean cultivation as well as other protein crops within the EU (FAOSTAT, 2024; Nendel et al., 2023; European Parliament, 2023). Within this framework, given the challenges posed by climate change and water scarcity, conducting WF assessment is imperative to ensure sustainable soybean production within the EU.

Considering the above-mentioned research gaps and to provide support to the EU in advocating science-based strategies to enhance soybean production, this study was undertaken to quantify the impacts of past and future climates on the WFs for soybean production in Italy and Slovenia. The present study aimed to firstly estimate the green and blue water volumes for soybean production in the baseline period (1981–2010) under both rainfed and irrigated conditions. For this approach, the various levels of readily available water (RAW) depletion within the effective root zone (ERZ) of soybean were considered as a threshold to start the irrigation. Secondly, the aim was to project the impacts of climate change on soybean blue and green water volumes in rainfed and irrigated conditions under three emission scenarios (SSP1-2.6, SSP2-4.5, and SSP5-8.5) and three future time periods (2041–2060, 2061–2080, 2081–2100). Lastly, the aim was to quantify and compare the dynamics of blue and green water volumes for soybean production in both the baseline period and future climates under both rainfed and irrigated conditions.

2 Methods and data

2.1 Study sites

The study sites were two locations in Italy (Castelfranco and Cesa) and one location in Slovenia (Ljubljana). Castelfranco is in the Veneto region (North-eastern Italy, 45° 41' 41.14" N, 11° 56' 44.89" E, 12 m a.s.l.) with a temperate humid subtropical climate (Köppen *Cfa*), whereas Cesa is in the Tuscany region (Central Italy, 43° 12' 29.32" N, 11° 50' 36.11" E, 249 m a.s.l.) and the climate is falls under the hot-summer Mediterranean type (Köppen *Csa*). Ljubljana is approximately in the central part of Slovenia with geographical coordinates of 46° 3′ N, 14° 30′ E, 295 m. a.s.l. The climate type is temperate, continental climate (Köppen *Cfb/Dfb*). Agronomic data were collected from the field experiments in Castelfranco and Cesa during the 2022 and 2023 growing seasons. For Ljubljana, data collection was performed for the 2015 and 2016 growing seasons. In 2022, the soybean growing period was from May 20 to October 4 and from June 16 to October 6 in Castelfranco and Cesa, respectively. In 2023, the growing period was from May 9 to October 4 in Cesa and from May 31 to October 9 in Castelfranco. In Ljubljana, the growing period in both years was from May 19 to October 3. The differences in the annual sowing dates for Italy was based primarily on the amount of rainfall. In Castelfranco, a total of 278 mm and 407 mm of rain was recorded during the 2022 and 2023 growing season, respectively. In Cesa, rainfall was 262 and 238 mm for the 2022 and 2023 growing season, respectively. In Ljubljana, a total of 287 mm and 336 mm of precipitations were recorded in 2015 and 2016, respectively.

Taking the 30-year (1981–2010) historical climate data, the seasonal (May–October) cumulative rainfall of Castelfranco, Cesa, and Ljubljana was 399 mm, 299 mm, and 588 mm, respectively. Furthermore, the seasonal minimum (T_{min}) and maximum (T_{max}) temperatures in Castelfranco were 15.1°C and 25.5°C, respectively. In Cesa, the T_{min} was 12.8°C whereas, the T_{max} was 26.0°C. In Ljubljana, the T_{min} was 12.1°C and the T_{max} was 22.8°C (Figure 1).

2.2 AquaCrop model and inputs

The AquaCrop model version 7.0 was used for the simulations. The comprehensive description of the model, along with the calculation scheme, can be found in the user guide, handbook, and pertinent publications (Raes et al., 2022; Raes, 2023; Steduto et al., 2009; Vanuytrecht et al., 2014). The model requires inputs related to climate, crop, soil, and field management which are discussed in detail in the subsequent sections.

2.2.1 Baseline and future climate scenarios

The historical climate data were extracted from the AGRI4CAST observational dataset, specifically from the grid cell

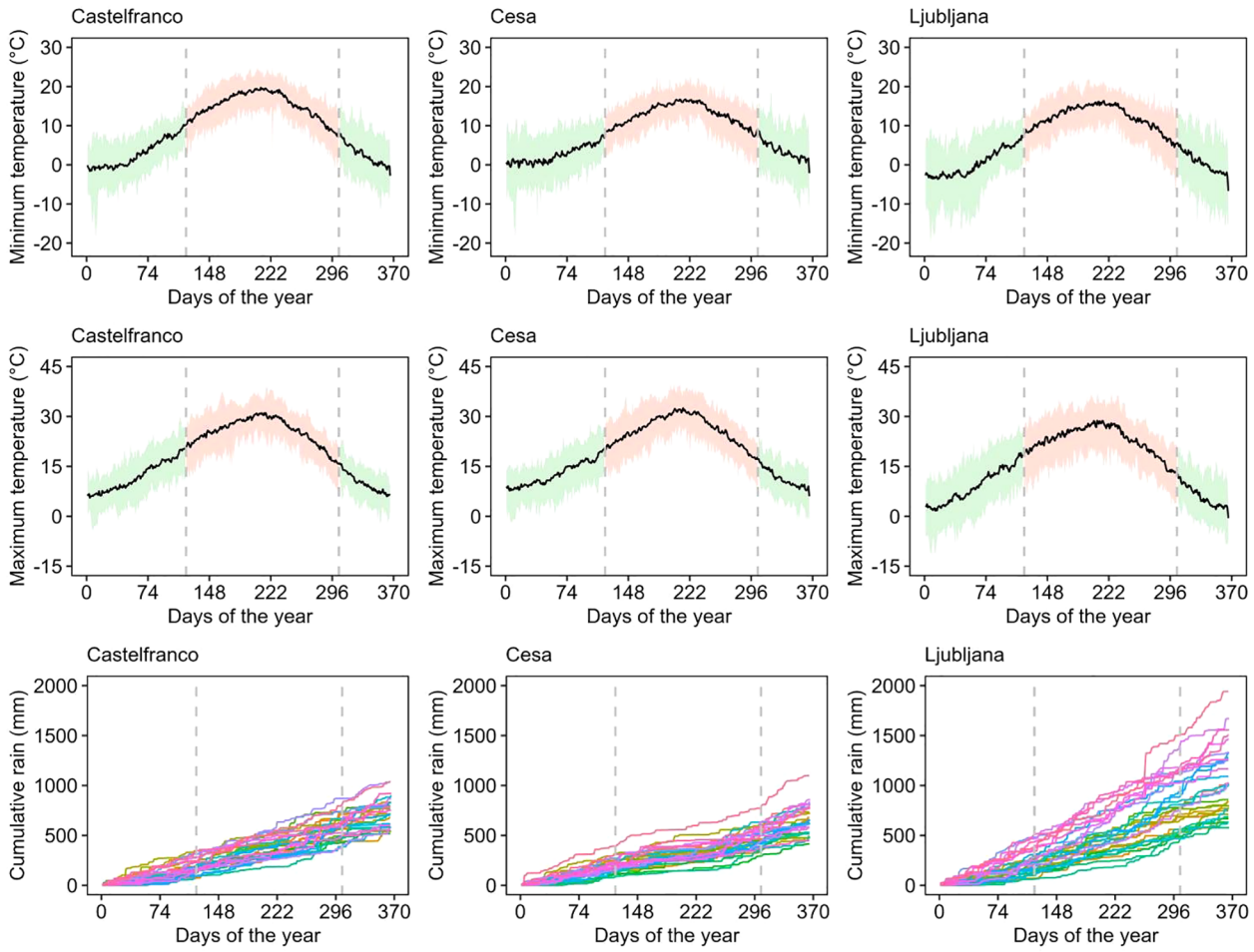

FIGURE 1
Historical climate data (1981–2010) of the study sites. The solid black line for minimum (T_{min}) and maximum (T_{max}) temperatures represents the 30-year daily average, whilst the coloured sections represent the minimum and maximum values both for the growing (pale orange) and non-growing seasons (pale green). The different line colors for cumulative rain represent each year from 1981 to 2010.

nearest to the respective geographical coordinates of each study site. The data were utilized to train the Long Ashton Research Station Weather Generator (LARS-WG) 7.0 (Semenov et al., 2002). Once trained, LARS-WG was used to generate 100 years of synthetic local-scale daily meteorological data (T_{min}, T_{max}, rainfall, solar radiation) for both the baseline period (1981–2010) and future climate scenarios. Specifically, three future time periods were considered: near future (2041–2060), mid-future (2061–2080), and far future (2081–2100). These time periods were considered along with three emission scenarios according to Shared Socio-economic Pathways (SSPs) (SSP1-2.6, SSP2-4.5, and SSP5-8.5), and three General Circulation Models (GCMs) (ACCESS-ESM1-5, HadGEM3-GC31-LL, and MRI-ESM2-0).

The SSP-based scenarios were used in the Coupled Model Intercomparison Project Phase 6 (CMIP6) which is the most recent set of climate model experiments. SSP1-2.6 (sustainable path), SSP2-4.5 (intermediate path), and SSP5-8.5 (fossil fuel-dominated development path) were chosen out of the five SSP families because they belong to the high priority scenarios according to the Intergovernmental Panel on Climate Change Sixth Assessment Report (IPCC AR6). Similarly, the three GCMs used were available from CMIP6 used in the recent IPCC AR6 and were selected because they are reliable to use with different emission scenarios and they are available GCMs in LARS-WG.

Synthetic time series produced with a weather generator does not represent actual weather but rather the potential realization of weather conditions within a given climate scenario. As such, the choice of 100 years was made to minimize the uncertainty in the stochastic generation of data by the weather generator, as it is recommended to use at least 60 years (Lawless and Semenov, 2005). The 100-year time series for baseline and future scenarios were then used as weather inputs for the crop model.

For all locations, the reference evapotranspiration (ET_o) was calculated on a daily basis using the Hargreaves equation (Equation 2), as described in "FAO Irrigation and Drainage Paper No. 56" (Allen et al., 1998), and then directly imported into the model. This method was used instead of the standard Penman-Monteith equation due to data limitations, and also because it is a recognized and accepted approach for estimating ET_o. The equation is as follows:

$$ET_{o,\ Har} = H_A \times R_e(T + 17.8) \times \Delta T^{H_E} \quad (2)$$

where H_A and H_E are standard values: H_A = 0.0023 and H_E = 0.5, R_e is the water equivalent of the radiation measured on the ground or terrestrial radiation (mm d^{-1}), T is the mean temperature ((T_{min} + T_{max})/2°C) and ΔT is the difference between maximum and minimum temperatures.

The average CO_2 concentration (366 ppm) used for the baseline period simulations was obtained from Meinshausen et al. (2017). Instead, the projections were based on SSPs in which the average CO_2 concentrations were obtained from Meinshausen et al. (2020). The summary of the meteorological variables is presented in Supplementary Table 1.

2.2.2 Soil parameters

Data from soil analyses at the respective study sites (Supplementary Table 2) were used as inputs to simulate the soil water movement and retention of water in the ERZ of soybean (Raes et al., 2022). The simulations were based on fine soil texture thus, neglecting the effects of the soil skeleton on the retention capacity and infiltration. Moreover, the groundwater table was not considered. This was based on the assumption that due to the depth of the groundwater table, it would have had negligible effects and that capillary rise would not have contributed moisture to the root zone.

2.2.3 Crop characteristics

The indicative values of crop parameters for soybean by Raes et al. (2022) and the agronomic data from the field experiments in the study sites were used to parametrize and calibrate the crop model (Supplementary Table 3). In the model, soybean was considered as a fruit or grain-producing crop with a yield formation period that started at flowering, coinciding with the progressive increase of the harvest index (HI). In the model, crop characteristics can be distinguished as either conservative or non-conservative. Thus, the cultivar-specific and non-conservative crop parameters were adjusted since they vary with the selected cultivar and may also be affected by field management, conditions in the soil profile, and climate. The parametrization and calibration were performed according to the user guide and procedure provided by Raes et al. (2022) and Vanuytrecht et al. (2014). Performance evaluation indicated that the AquaCrop model successfully simulated soybean grain yield in the study sites.

2.2.4 Irrigation

The simulations were conducted under both rainfed and irrigated conditions. Various levels of RAW depletion within the soybean ERZ were considered as thresholds to start the irrigation. These RAW depletion thresholds ranged from 25%, 50%, 75% to 100%. In this study, these are referred to as irrigation strategies and were evaluated in terms of change in yield and WF in relation to climate change. The maximum effective rooting depth in Castelfranco and Cesa was 1.0 m, whereas it was 0.70 m in Ljubljana. It is important to note that the depletion considered in the simulations was the RAW in the root zone and not the total available water between field capacity and the permanent wilting point. An irrigation file was created for each irrigation strategy by specifying each threshold in the root zone. That means that if the threshold was reached, irrigation was added to the soil profile to keep the moisture in the ERZ above the threshold. Thus, the total irrigation added to the soil profile throughout the growing period constitutes the net irrigation requirements (NIR) of soybean (Raes et al., 2022). On the other hand, no irrigation file was created for the rainfed conditions since it represented the default in AquaCrop.

2.3 Model application

For each location, packaged project files were created using the 100-year time series produced with LARS-WG as weather input for the AquaCrop model. Simulations were performed under both rainfed and irrigated conditions by considering both the irrigation strategies mentioned previously and the crop characteristics (e.g. thermal requirements) of the field experiments conducted in the respective study sites. Simulations were performed under Growing Degree Days (GDD) mode and with the initial condition of the soil water profile set at field capacity, allowing the simulations to provide optimal conditions for crop germination and establishment. Moreover, the initial soil water content consumed by the crop on the first day was assumed to be green water based on the soil water balance model (Gao et al., 2023). Sowing dates were standardized across all simulations based on the first growing season: May 20 for Castelfranco, June 16 for Cesa, and May 19 for Ljubljana. In order to avoid carry-over effects, soil conditions were re-initialized at the beginning of each simulation year. The details of the simulation and calculation procedures are discussed in the succeeding sections.

2.3.1 Simulation of daily evapotranspiration

The AquaCrop model assumes that the crop grows under optimal conditions, in that crop water demand is fully satisfied. It simulates daily ET_c (mm) using the two-step approach by multiplying the crop coefficient (K_c) by ET_o (Equation 3). The dual K_c (Equation 4) consists of a basal crop coefficient (K_{cb}) and an evaporation coefficient (K_e) (Allen et al., 1998; Pereira et al., 2015).

$$ET_c = K_c * ET_o \quad (3)$$

$$K_c = K_{cb} + K_e \quad (4)$$

where K_{cb} and K_e are related to the portion of crop transpiration (T_c) and soil evaporation (E_s) over ET_o, respectively.

In this study, the irrigation and rainfall were assumed to be the only sources of blue and green WFs, respectively. As mentioned previously, the contribution of blue water from capillary rise was not taken into consideration due to negligible effects from the groundwater table. By tracking the proportion of daily rainfall and irrigation added to the soil profile under rainfed and irrigated conditions, the daily ET_c of soybean was divided into $ET_{c\text{-}blue}$ and $ET_{c\text{-}green}$ as described in the following section.

2.4 Estimation of soybean blue and green water footprints

This study specifically focused on the direct blue and green WFs associated with soybean cultivation in the field, as they are mainly affected by climate and crop water use. The indirect WFs from other inputs in crop production were excluded. Exclusion factors included machinery and energy use (Zhuo et al., 2016a) as well as grey WF, mainly dependent on pollution and water quality. Within the framework of WFs, yield attributable to blue and green water was calculated. It is described as the amount of water in m^3 necessary to produce a ton of harvested yield per hectare, and was calculated according to Equation 5 (Bocchiola et al., 2013; Chukalla et al., 2015; Gao et al., 2023; Mekonnen and Hoekstra, 2011) provided below:

$$WF_{blue,green} = \left(\frac{10*CWR_{blue}}{Y}\right) \text{ or } \left(\frac{10*CWR_{green}}{Y}\right) \quad (5)$$

where $WF_{blue,green}$ (m^3 ton^{-1}) is the blue or green WF, CWR_{blue} and CWR_{green} are the blue and green crop water requirements (CWR) in mm, respectively, 10 is a conversion factor from mm to m^3, and Y is the total crop yield (ton ha^{-1}) produced per growing period.

In this study, $WF_{blue,green}$ is interpreted as blue or green WF in terms of soybean dry grain yield.

2.4.1 Estimation of soybean blue and green crop water requirements

The sum of the daily ET_c for the entire crop growth period is equivalent to CWR (Pereira and Alves, 2013). Thus, the CWRs under rainfed ($CWR_{rainfed}$) and irrigated ($CWR_{irrigated}$) conditions were calculated for the crop growth period according to Equation 6 and Equation 7 as shown below. The CWR was based on the cumulative values of the corresponding daily ET_c under rainfed ($ET_{c\text{-}rainfed}$) and irrigated ($ET_{c\text{-}irrigated}$) conditions, respectively, as simulated by AquaCrop.

$$CWR_{rainfed} = \sum_{d=1}^{gp} ET_{c-rainfed} \quad (6)$$

$$CWR_{irrigated} = \sum_{d=1}^{gp} ET_{c-irrigated} \quad (7)$$

where gp is the duration of the soybean growing period (days) and d=1 is the day of sowing.

Under rainfed conditions, the amount of water that undergoes evapotranspiration is derived solely from the rainfall. Therefore, the green water (CWR_{green}) is equivalent to $CWR_{rainfed}$ (Equation 8). On the other hand, the evapotranspiration under irrigated conditions is derived from both rainfall and irrigation. As such, the $CWR_{irrigated}$ is equal to the sum of blue water (CWR_{blue}) and CWR_{green} (Equation 9). Therefore, CWR_{blue} can be derived from the difference between $CWR_{irrigated}$ and $CWR_{rainfed}$ (Equation 10) (Ventrella et al., 2017).

$$CWR_{rainfed} = CWR_{green} \quad (8)$$

$$CWR_{irrigated} = CWR_{blue} + CWR_{green} \quad (9)$$

$$CWR_{blue} = CWR_{irrigated} - CWR_{rainfed} \quad (10)$$

2.4.2 Estimation of water footprints under rainfed and irrigated conditions

The only source of water under rainfed conditions is rainfall. Thus, the consumptive WFs throughout the growing period ($WF_{rainfed}$) are equivalent to WF_{green} (Equation 11). On the other hand, under irrigated conditions, the source of water is derived from both rainfall and irrigation. Thus, the consumptive WFs under irrigated conditions ($WF_{irrigated}$) are equivalent to the sum of WF_{blue} and WF_{green} (Equation 12).

$$WF_{rainfed} = WF_{green} \quad (11)$$

$$WF_{irrigated} = WF_{blue} + WF_{green} \quad (12)$$

2.5 Post-processing of AquaCrop output and data analysis

The simulation results were post-processed to calculate the seasonal blue and green CWRs and WFs, and total WFs under rainfed and irrigated conditions using the aforementioned equations. The calculations were performed for both baseline and future climates across locations. The results of the calculations were analyzed considering the locations, irrigation strategies, SSPs, and time periods (only for the future climate) as the main factors. Accordingly, their variations were compared using ANOVA followed by *post-hoc* analysis using Tukey's Honest Significant Difference (HSD) to compare differences between means. Statistical tests were performed at α = 0.01 using the open-source statistical software jamovi©, whereas the library (ggplot2) in R was used for data visualizations (R Core Team, 2021). Finally, the impact of the irrigation strategies was evaluated in terms of the percentage change in yield and consumptive WFs relative to rainfed conditions for both the baseline and future climates. Instead, the impact of climate change was evaluated by comparing the yield and consumptive WFs of SSPs with the baseline for both rainfed and irrigated conditions. The values were normalized and as such should be interpreted as the percentage difference relative to the baseline period for climate change impacts. For the impacts of irrigation strategies, values should be interpreted as the percentage difference relative to rainfed conditions.

3 Results

3.1 Water footprints and water use for soybean production in the baseline period

3.1.1 $WF_{rainfed}$ and green water

The estimated $WF_{rainfed}$ and green water for soybean production across the study sites in the baseline period are presented in Figure 2 and

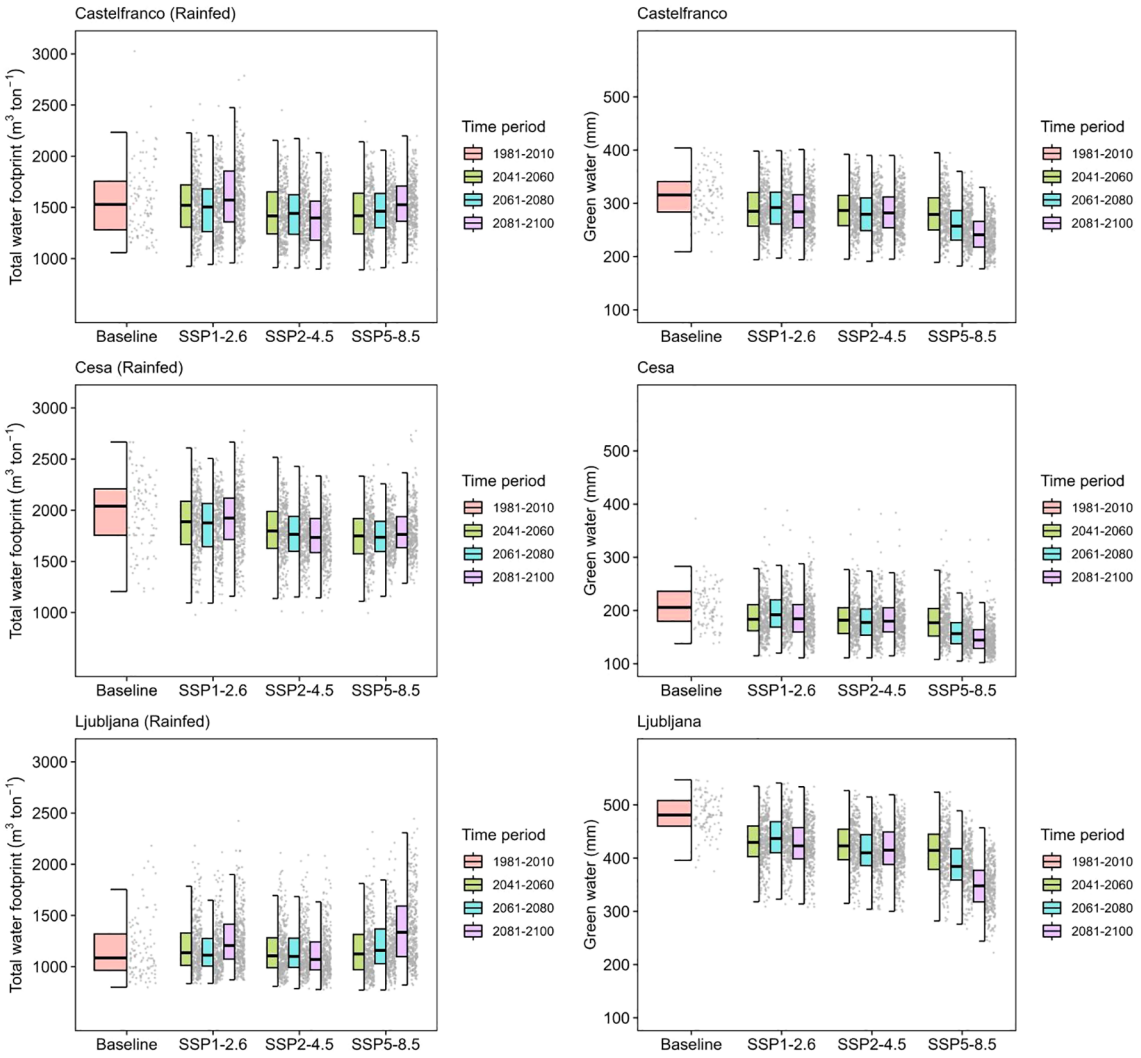

FIGURE 2
Consumptive water footprints (m^3 ton^{-1}) under rainfed conditions ($WF_{rainfed}$) and green water (mm) of the study sites across different SSPs and time periods.

Table 1. The $WF_{rainfed}$ varied significantly across locations ($p < 0.01$) and was the highest in Cesa (1984 m^3 ton^{-1}), followed by Castelfranco (1570 m^3 ton^{-1}) and Ljubljana (1178 m^3 ton^{-1}), respectively.

The green water varied significantly across locations with an average of 315 mm in Castelfranco, 209 mm in Cesa, and 481 mm in Ljubljana. The ANOVA showed that the rainfall varied significantly across locations ($p < 0.01$). Thus, Ljubljana having the highest seasonal cumulative rainfall registered the highest green water. Similarly, Cesa had the lowest rainfall and, accordingly registered the lowest green water (Supplementary Table 1). The highest estimated grain yield under rainfed conditions was observed in Ljubljana, followed by Castelfranco, and finally Cesa (Supplementary Table 4). Thus, Ljubljana, with the highest green water and yield, registered the lowest $WF_{rainfed}$.

3.1.2 $WF_{irrigated}$, blue WF, and blue water

The estimated $WF_{irrigated}$, blue WF, and blue water of the respective study sites in the baseline period are presented in Figure 3 and Tables 1–3. Under irrigated conditions, the $WF_{irrigated}$ was equivalent to the sum of green and blue WFs. The results showed that soybean production relied primarily on green WF, contributing to about 68.3 to 100% of the consumptive WFs, whereas the blue WF contribution ranged from 0 to 31.7%. The $WF_{irrigated}$ was only significantly different across locations ($p < 0.01$) and was not significant across irrigation strategies ($p = 0.08$). The $WF_{irrigated}$ ranged from 1922 to 1976 m^3 ton^{-1} in Castelfranco, from 2535 to 2694 m^3 ton^{-1} in Cesa, and from 1295 to 1339 m^3 ton^{-1} in Ljubljana.

The blue WF was significantly different across both irrigation strategies and locations ($p < 0.01$). In all locations, the 25% RAW depletion registered the highest blue WF with an average of 406, 710, and 161 m^3 ton^{-1} in Castelfranco, Cesa, and Ljubljana, respectively. Conversely, the lowest blue WF was observed at 100% RAW depletion with an average of 352, 552, and 118 m^3 ton^{-1} in Castelfranco, Cesa, and Ljubljana, respectively (Table 2). Considering the blue WF reduction, the results showed that up to 50% RAW depletion can be implemented in Castelfranco and Cesa

10.3389/fagro.2026.1748798

TABLE 1 Consumptive water footprints (m^3 ton^{-1}) under irrigated ($WF_{irrigated}$) and rainfed ($WF_{rainfed}$) conditions for the baseline period and future scenarios (SSP1-2.6, SSP2-4.5, and SSP5-8.5) across three time periods.

Locations	*Irrigation strategies	**Time periods									
		1981–2010	2041–2060			2061–2080			2081–2100		
	Allowable depletion	Baseline	SSP1-2.6	SSP2-4.5	SSP5-8.5	SSP1-2.6	SSP2-4.5	SSP5-8.5	SSP1-2.6	SSP2-4.5	SSP5-8.5
Castelfranco	100% RAW	1922^{ak}	1894^{al}	1806^{am}	1796^{an}	1868^{ao}	1804^{bp}	1855^{aq}	1998^{ar}	1739^{bs}	1970^{at}
	75% RAW	1945^{ck}	1917^{cl}	1831^{cm}	1817^{cn}	1895^{co}	1827^{cp}	1875^{cq}	2023^{cr}	1762^{ds}	1985^{ct}
	50% RAW	1965^{ek}	1926^{el}	1839^{em}	1823^{fn}	1904^{eo}	1834^{fp}	1875^{eq}	2029^{er}	1770^{fs}	1980^{et}
	25% RAW	1976^{gk}	1937^{gl}	1849^{gm}	1833^{hn}	1914^{go}	1843^{hp}	1883^{gq}	2039^{gr}	1779^{hs}	1988^{gt}
	Rainfed	1570^{i}	1524^{i}	1455^{i}	1439^{i}	1508^{i}	1446^{i}	1470^{i}	1604^{i}	1398^{j}	1541^{i}
Cesa											
	100% RAW	2535^{ak}	2477^{al}	2393^{an}	2336^{bp}	2421^{aq}	2355^{bs}	2407^{au}	2538^{av}	2300^{bx}	2539^{az}
	75% RAW	2635^{ck}	2559^{clm}	2472^{dno}	2407^{dp}	2509^{cqr}	2444^{dst}	2462^{du}	2615^{cvw}	2379^{dxy}	2579^{cz}
	50% RAW	2665^{ek}	2573^{elm}	2484^{fno}	2418^{fp}	2526^{er}	2439^{fst}	2460^{fu}	2629^{evw}	2391^{fxy}	2570^{ez}
	25% RAW	2694^{gk}	2597^{hm}	2507^{ho}	2440^{hp}	2551^{hr}	2461^{ht}	2477^{hu}	2653^{gw}	2412^{hy}	2584^{gz}
	Rainfed	1984^{i}	1877^{i}	1805^{j}	1749^{j}	1853^{i}	1768^{j}	1747^{j}	1914^{i}	1738^{j}	1800^{j}
Ljubljana											
	100% RAW	1295^{ak}	1379^{al}	1339^{am}	1376^{an}	1339^{ao}	1349^{ap}	1445^{bq}	1474^{br}	1309^{as}	1672^{bt}
	75% RAW	1318^{ck}	1402^{cl}	1361^{cm}	1396^{cn}	1362^{co}	1369^{cp}	1465^{dq}	1497^{dr}	1331^{cs}	1692^{dt}
	50% RAW	1331^{ek}	1413^{el}	1372^{em}	1405^{en}	1373^{eo}	1380^{ep}	1472^{fq}	1508^{fr}	1340^{es}	1692^{ft}
	25% RAW	1339^{gk}	1420^{gl}	1379^{gm}	1412^{gn}	1380^{go}	1386^{gp}	1477^{hq}	1515^{hr}	1347^{gs}	1697^{ht}
	Rainfed	1178^{ik}	1196^{i}	1159^{i}	1179^{i}	1168^{i}	1158^{i}	1219^{i}	1268^{i}	1130^{i}	1378^{j}

The values are derived from simulations using 100-year synthetic weather data and three General Circulation Models (GCMs) for the future scenarios.
*values across irrigation strategies in the baseline and SSPs in each time period with the same letter were not significantly different.
**values across SSPs in each time period with the same letter as the baseline were not significantly different.

without a significant reduction in grain yield. In Ljubljana, the RAW depletion can be increased up to 75%.

Generally, all locations showed an increasing pattern of blue water as the allowable RAW depletion decreased, although this was not as apparent in Ljubljana (Table 3). The ANOVA revealed significant variation in blue water across different irrigation strategies and locations ($p < 0.01$). In Castelfranco, the blue water ranged from 165 to 214 mm whereas, from 141 to 226 mm in Cesa, and from 66 to 101 mm in Ljubljana.

3.2 Water footprints and water use for soybean production under climate change scenarios

3.2.1 $WF_{rainfed}$ and green water

The $WF_{rainfed}$ and green water for soybean production in the study sites across the SSPs and future time periods are presented in Figure 2 and Table 1. In Castelfranco, the $WF_{rainfed}$ ranged from 1398 to 1604 m^3 ton^{-1}, whereas it ranged from 1738 to 1914 m^3 ton^{-1} in Cesa and from 1130 to 1378 m^3 ton^{-1} in Ljubljana. In Castelfranco and Cesa, climate change reduced the $WF_{rainfed}$ as indicated by the lower values in SSPs compared to the baseline. The exception was for SSP1-2.6 in the far future in Castelfranco. In contrast, $WF_{rainfed}$ remained relatively stable in Ljubljana, although an increase was observed in the far future under SSP1-2.6 and SSP5-8.5.

Ljubljana had the highest green water, ranging from 347 to 438 mm followed by Castelfranco (243–293 mm) and Cesa (149–196 mm), respectively. Across the SSPs, the same pattern was observed in all locations which coincided with the trend in rainfall. The green water was relatively stable under SSP1-2.6 and SSP2-4.5 across time periods but was shown to decrease under SSP5-8.5.

The lowest $WF_{rainfed}$ was observed in Ljubljana due to high green water, yield, and rainfall. Instead, Cesa had a higher $WF_{rainfed}$ compared to the remaining two sites due to low green water, yield, and rainfall (Supplementary Tables 1, 4).

3.2.2 $WF_{irrigated}$, blue WF, and blue water

The $WF_{irrigated}$ of each study site across the SSPs and time periods is presented in Figure 3 and Table 1. In Castelfranco, the $WF_{irrigated}$ ranged from 1739 to 2039 m^3 ton^{-1}, from 2300 to 2653 m^3

10.3389/fagro.2026.1748798

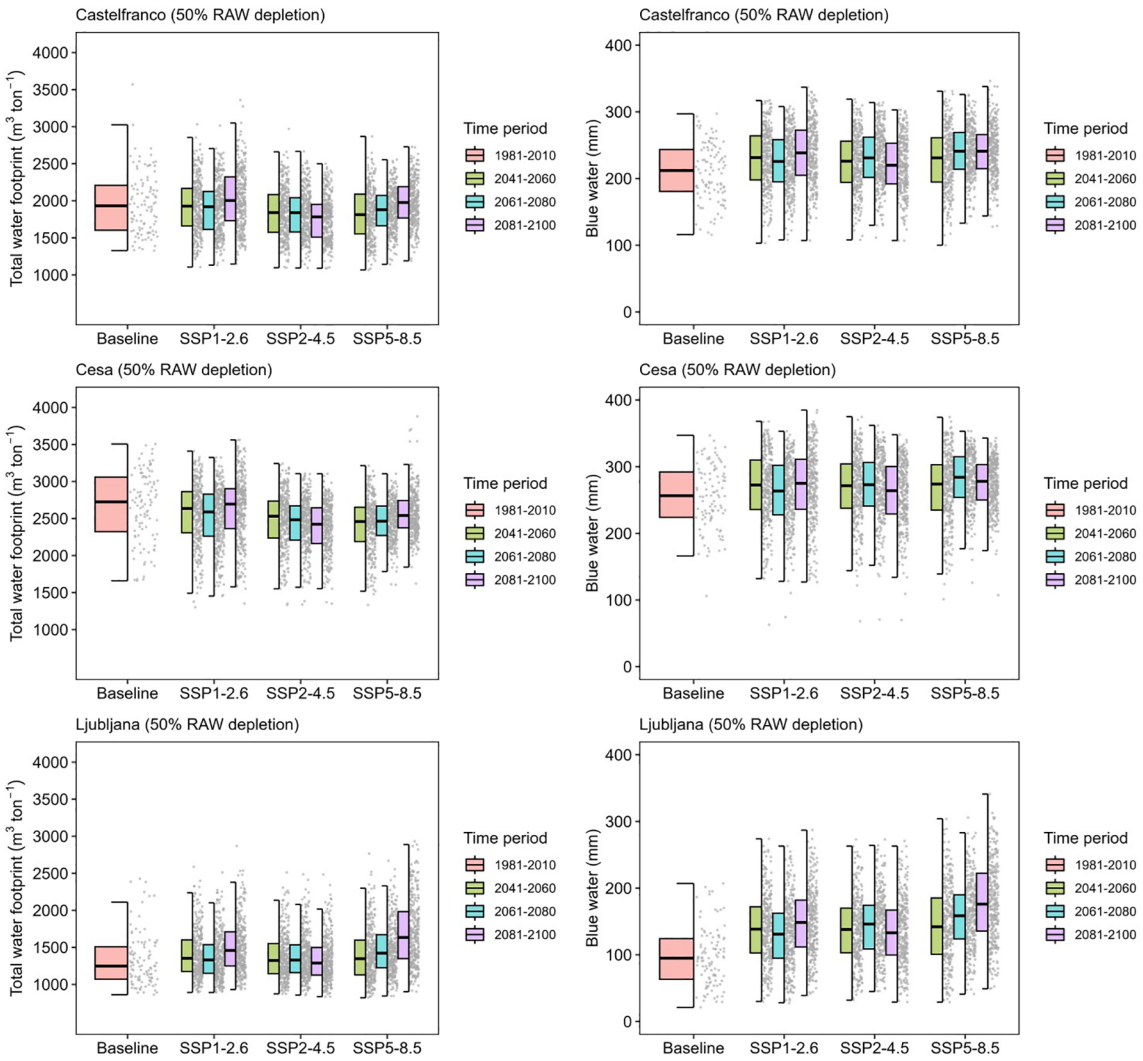

FIGURE 3
Consumptive water footprints (m^3 ton^{-1}) under irrigated ($WF_{irrigated}$) and blue water (mm) of the study sites under irrigated conditions [50% readily available water (RAW) depletion] across different SSPs and time periods.

ton^{-1} in Cesa, and from 1309 to 1697 m^3 ton^{-1} in Ljubljana. The green WF constituted a significant portion of the consumptive WFs for soybean production, and ranged from 69.9 to 87.8% in Castelfranco, 59.6 to 94.5% in Cesa, and 70.9 to 100% in Ljubljana. In contrast, the contribution of blue WF accounted for approximately 12.2 to 30.1% of the consumptive WFs in Castelfranco, 5.5 to 40.4% in Cesa, and 0 to 29.1% in Ljubljana.

In Castelfranco, climate change reduced the $WF_{irrigated}$ as indicated by lower values in SSPs compared to the baseline. The exception was noted for the far future under SSP1-2.6 and SSP5-8.5. Climate change also reduced the $WF_{irrigated}$ in Cesa, but caused an increase in Ljubljana. All locations followed the same dynamics of $WF_{irrigated}$ among the SSPs across time periods. Under SSP5-8.5, the $WF_{irrigated}$ is expected to increase from the near to far future. Conversely, a reduction in $WF_{irrigated}$ is expected under SSP2-4.5. Instead in Ljubljana, a slight increase was observed from the near to mid-future. Under SSP1-2.6, a decrease and increase in $WF_{irrigated}$ is expected from the near to mid-future and from the mid to far future, respectively.

The $WF_{irrigated}$ across irrigation strategies did not vary significantly in Castelfranco and Ljubljana. However, in Cesa, the $WF_{irrigated}$ at 100% RAW depletion was significantly lower than the other irrigation strategies. In all locations, the same trend of increasing $WF_{irrigated}$ was observed as the allowable RAW depletion decreased. The highest $WF_{irrigated}$ was observed at 25% RAW depletion, and ranged from 1779 to 2039 m^3 ton^{-1} in Castelfranco, from 2412 to 2653 m^3 ton^{-1} in Cesa, and from 1347 to 1697 m^3 ton^{-1} in Ljubljana. Conversely, the lowest $WF_{irrigated}$ was observed at 100% RAW depletion, ranging from 1739 to 1998 m^3 ton^{-1} in Castelfranco, from 2300 to 2539 m^3 ton^{-1} in Cesa, and from 1309 to 1672 m^3 ton^{-1} in Ljubljana.

The blue WF of each study site across the SSPs and time periods is presented in Table 2. The highest blue WF (561–784 m^3 ton^{-1}) was observed in Cesa, followed by Castelfranco (341–447 m^3 ton^{-1}), and Ljubljana (171–319 m^3 ton^{-1}), respectively. The dynamics of

10.3389/fagro.2026.1748798

TABLE 2 Blue water footprint (m^3 ton^{-1}) under irrigated conditions (WF_{blue}) for the baseline period and future scenarios (SSP1-2.6, SSP2-4.5, and SSP5-8.5) across three time periods.

Locations	*Irrigation strategies	**Time periods									
		1981–2010	2041–2060			2061–2080			2081–2100		
Castelfranco	Allowable depletion	Baseline	SSP1-2.6	SSP2-4.5	SSP5-8.5	SSP1-2.6	SSP2-4.5	SSP5-8.5	SSP1-2.6	SSP2-4.5	SSP5-8.5
	100% RAW	352^{as}	369^{a}	352^{a}	357^{aj}	360^{a}	358^{a}	385^{b}	394^{b}	341^{a}	429^{bq}
	75% RAW	374^{crs}	393^{ci}	376^{ci}	378^{cjk}	387^{cl}	381^{cm}	405^{dn}	419^{do}	364^{cp}	444^{dq}
	50% RAW	395^{er}	402^{ei}	385^{ei}	385^{ek}	396^{el}	388^{em}	405^{en}	425^{eo}	372^{ep}	439^{fq}
	25% RAW	406^{gr}	412^{gi}	395^{gi}	394^{gk}	406^{gl}	397^{gm}	414^{gn}	435^{go}	381^{gp}	447^{hq}
Cesa											
	100% RAW	552^{a}	600^{a}	588^{a}	587^{a}	567^{a}	587^{a}	660^{b}	623^{b}	561^{a}	739^{bt}
	75% RAW	652^{cv}	683^{cj}	667^{ck}	657^{cl}	656^{cn}	676^{co}	714^{dp}	700^{cr}	641^{cs}	779^{du}
	50% RAW	682^{ev}	696^{eij}	679^{ek}	668^{el}	673^{emn}	671^{eo}	713^{ep}	714^{eqr}	652^{es}	770^{ftu}
	25% RAW	710^{gv}	721^{gij}	702^{gk}	690^{gl}	697^{gm}	693^{go}	730^{gp}	739^{gq}	674^{gs}	784^{hu}
Ljubljana											
	100% RAW	118^{av}	184^{b}	180^{bj}	196^{bl}	171^{b}	192^{b}	226^{bo}	205^{bq}	180^{bs}	295^{bu}
	75% RAW	141^{cvw}	206^{di}	202^{djk}	217^{dlm}	194^{dn}	212^{dn}	246^{dop}	228^{dqr}	201^{dst}	314^{du}
	50% RAW	154^{evw}	218^{fi}	213^{fk}	226^{fm}	205^{fn}	222^{fn}	253^{fp}	239^{fr}	210^{ft}	314^{fu}
	25% RAW	161^{gw}	225^{hi}	220^{hk}	233^{hm}	213^{hn}	229^{hn}	259^{hp}	247^{hr}	217^{ht}	319^{hu}

The values are derived from simulations using 100-year synthetic weather data and three General Circulation Models (GCMs) for the future scenarios.
*values across irrigation strategies in the baseline and SSPs in each time period with the same letter were not significantly different.
**values across SSPs in each time period with the same letter as the baseline were not significantly different.

blue WF among the SSPs across time periods followed the same pattern as $WF_{irrigated}$. In all locations, the blue WF is expected to increase from the near to far future under SSP5-8.5. On the other hand, it is expected to decrease from mid to far future under SSP2-4.5. Using the same emission scenario, blue WF is expected to increase from the near to mid-future, except in Cesa. Finally, under SSP1-2.6, the blue WF is expected to decrease from the near to mid future and increase from the mid to far future.

In all locations, the highest blue WF among irrigation strategies was observed at 25% RAW depletion, and ranged from 381 to 447 m^3 ton^{-1} in Castelfranco, from 674 to 784 m^3 ton^{-1} in Cesa, and from 213 to 319 m^3 ton^{-1} in Ljubljana. Consequently, the lowest average blue WF was observed at 100% RAW depletion, and ranged from 341 to 429 m^3 ton^{-1} in Castelfranco, 561 to 739 m^3 ton^{-1} in Cesa, and 171 to 295 m^3 ton^{-1} in Ljubljana.

The blue water varied significantly across locations, SSPs, and irrigation strategies (Figure 3, Table 3). In Castelfranco, the blue water ranged from 175 to 244 mm, from 147 to 289 mm in Cesa, and from 97 to 180 mm in Ljubljana. In all locations, the blue water increased under climate change scenarios. The increases were prominent under SSP5-8.5 in the mid or far future, although some variability did exist.

The dynamics of blue water across irrigation strategies followed the same pattern as $WF_{irrigated}$. In all locations, the highest average blue water was observed at 25% RAW depletion. Values ranged from 225 to 244 mm in Castelfranco, from 270 to 289 mm in Cesa, and from 135 to 180 mm in Ljubljana. Consequently, the lowest average blue water was observed at 100% RAW depletion, and ranged from 175 to 195 mm, 147 to 162 mm and 97 mm to 144 mm in Castelfranco, Cesa and Ljubljana, respectively.

3.3 Relative changes in yield and consumptive water footprints

3.3.1 Baseline period

The relative changes in yield and consumptive WFs were both positive indicating that irrigation increased the soybean yield with a proportionate increase in consumptive WFs depending on allowable depletion of RAW. There were noticeable differences in yield increases between 100% RAW depletion and other irrigation strategies, particularly evident for Cesa. The yield increases in Castelfranco (121.3–148.8%) and Ljubljana (36.6–50.1%) across irrigation strategies were relatively stable compared to Cesa (137.8–239.9%). In contrast, the change in consumptive WFs across all irrigation strategies remained relatively uniform in each location. Values ranged from 22.4 to 25.9% in Castelfranco, 27.8 to 35.8% in Cesa, and 9.9 to 13.7% in Ljubljana.

3.3.2 Future climate scenarios

The changes in yield and consumptive WFs of the various irrigation strategies relative to rainfed conditions are presented in

10.3389/fagro.2026.1748798

TABLE 3 Blue water (mm) under irrigated conditions for the baseline period and future scenarios (SSP1-2.6, SSP2-4.5, and SSP5-8.5) across three time periods.

Locations	*Irrigation strategies	**Time periods									
		1981–2010	2041–2060			2061–2080			2081–2100		
Castelfranco	Allowable depletion	Baseline	SSP1-2.6	SSP2-4.5	SSP5-8.5	SSP1-2.6	SSP2-4.5	SSP5-8.5	SSP1-2.6	SSP2-4.5	SSP5-8.5
	100% RAW	165^{a}	182^{b}	177^{a}	182^{b}	176^{a}	183^{b}	192^{b}	187^{b}	175^{a}	195^{b}
	75% RAW	189^{c}	211^{d}	207^{d}	211^{d}	207^{d}	213^{d}	224^{d}	219^{d}	204^{c}	226^{d}
	50% RAW	209^{er}	230^{fi}	225^{ej}	229^{fk}	225^{fl}	231^{fm}	241^{fn}	237^{fo}	221^{ep}	241^{fq}
	25% RAW	214^{gr}	234^{hi}	229^{gj}	233^{hk}	229^{hl}	235^{hm}	244^{hn}	242^{ho}	225^{gp}	244^{hq}
Cesa											
	100% RAW	141^{a}	151^{a}	151^{a}	153^{a}	147^{a}	154^{a}	162^{b}	153^{a}	150^{a}	160^{b}
	75% RAW	220^{c}	235^{c}	234^{c}	234^{c}	227^{c}	250^{d}	249^{d}	237^{d}	228^{c}	244^{d}
	50% RAW	255^{ei}	269^{ej}	268^{ek}	267^{el}	260^{em}	269^{en}	281^{fo}	271^{fp}	260^{eq}	274^{fr}
	25% RAW	266^{gi}	279^{gj}	278^{gk}	277^{gl}	271^{gm}	279^{gn}	289^{ho}	281^{gp}	270^{gq}	282^{gr}
Ljubljana											
	100% RAW	66^{az}	104^{b}	104^{b}	111^{b}	97^{b}	111^{b}	125^{b}	112^{b}	103^{b}	144^{b}
	75% RAW	85^{czb}	126^{dj}	125^{dl}	134^{dn}	118^{dpq}	132^{d}	147^{dt}	135^{dv}	125^{dx}	168^{dy}
	50% RAW	97^{eb}	139^{fij}	138^{fkl}	146^{fmn}	130^{foq}	145^{fr}	159^{fst}	148^{fuv}	135^{fwx}	178^{fy}
	25% RAW	101^{gb}	143^{hi}	142^{hk}	150^{hm}	135^{hop}	148^{hr}	162^{hs}	152^{hu}	139^{hw}	180^{hy}

The values are derived from simulations using 100-year synthetic weather data and three General Circulation Models (GCMs) for the future scenarios.
*values across irrigation strategies in the baseline and SSPs in each time period with the same letter were not significantly different.
**values across SSPs in each time period with the same letter as the baseline were not significantly different.

Figure 4. In all locations, the magnitude of change was determined by the RAW depletion. The lowest changes were evident at 100% RAW depletion, and the highest between 25% and 50% RAW depletion with negligible differences. The relative yield change in Castelfranco (140.2–236.9%) was comparable with that of Cesa (141.5–329.4%), whereas it was substantially lower in Ljubljana (42.4–109.4%). Across the irrigation strategies, the trend was the same in Castelfranco and Ljubljana with minimal differences. Notably, in Cesa, the change in yield was prominent at 100% RAW depletion and was significantly different from the three other irrigation strategies. Consequently, the increased yield across irrigation strategies coincided with a proportional increase in consumptive WFs. These values ranged from 23.9 to 29.0%, 30.7 to 43.6% and 14.6 to 23.1% in Castelfranco, Cesa and Ljubljana, respectively. In all locations, the increase in consumptive WFs was relatively uniform across strategies and followed the same trend as the relative yield change.

The change in yield and consumptive WFs of the various SSPs relative to the baseline is presented in Figure 4. Under rainfed conditions, climate change reduced soybean grain yield by -23.7 to -0.28% in Castelfranco, -24.3 to -0.63% in Cesa, and -37.1 to -9.4% in Ljubljana. Under irrigated conditions, the relative change in yield in Castelfranco and Cesa across the SSPs was generally positive, except for the far future under SSP5-8.5 in Cesa. The change in yield was negligent to negative in Ljubljana regardless of the SSPs and time periods. The change in yield under irrigated conditions ranged from -2.4 to 12.2% in Castelfranco, -15.7 to 9.2% in Cesa, and -14.9 to 0.32% in Ljubljana. The magnitude of change was dependent on the SSPs, which were the highest and lowest under SSP5-8.5 and SSP2-4.5, respectively. A notable yield reduction was observed in the far future under SSP5-8.5 in both Cesa (-15.7 to -4.4%) and Ljubljana (-14.9 to -12.1%). Regardless of whether the cultivations were irrigated or rainfed, climate change reduced the WF of Castelfranco and Cesa. The exception was for the far future under SSP1-2.6 and SSP5-8.5 in Castelfranco, where a minimal increase was observed. Conversely, consumptive WFs generally increased in Ljubljana under both rainfed and irrigated conditions. The relative change in consumptive WFs ranged from -11.0 to 4.0% in Castelfranco, -12.4 to 0.16% in Cesa, and -4.1 to 29.1% in Ljubljana. In all locations, the change in consumptive WFs among SSPs was relatively uniform in each time period and followed the opposite trend to the relative change in yield.

4 Discussion

4.1 Water footprints and water use in the baseline period

To understand the potential impacts of climate change on soybean production and WFs in the past, we performed simulations using the baseline climate data from 1981 to 2010

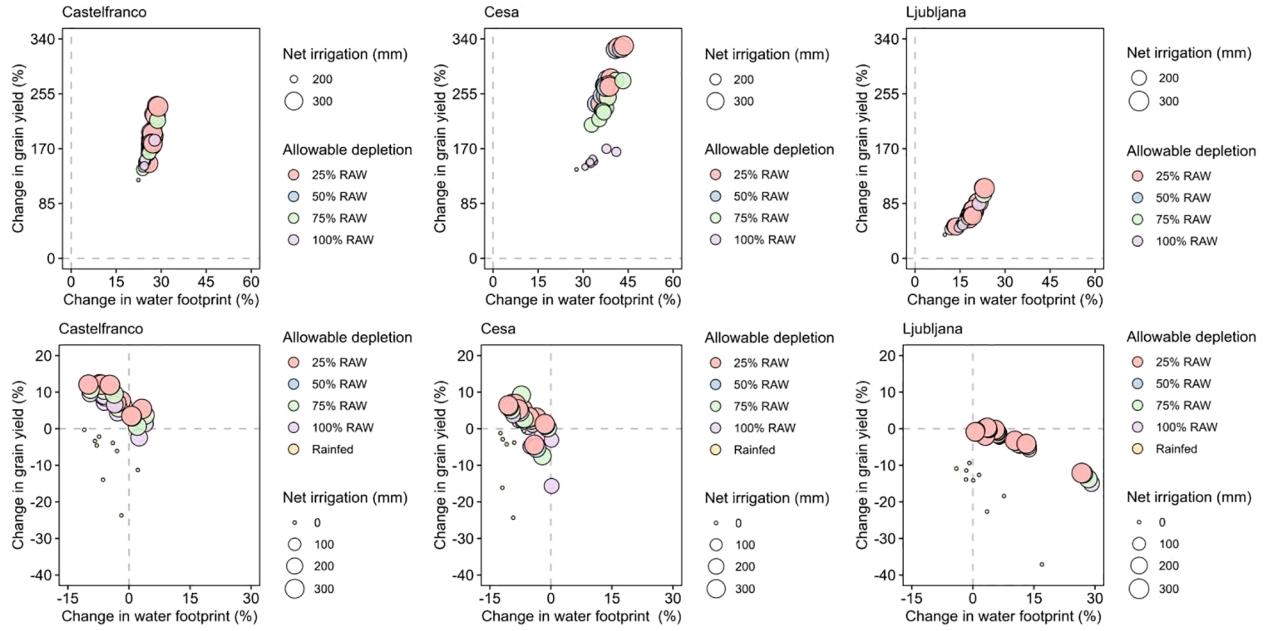

FIGURE 4
Change in dry grain yield and consumptive water footprints (%) of various irrigation strategies, relative to the rainfed conditions (upper panel) and relative to the baseline period (lower panel) across study sites. The horizontal and vertical grey dashed lines represent zero reference. Net irrigation or NIR constitutes the total irrigation added to the soil profile throughout the growing period.

under rainfed and irrigated systems. The $WF_{rainfed}$ was the highest in Cesa which signified that less green water was available to produce an equivalent amount of soybean grain yield per hectare than that shown for Castelfranco and Ljubljana, respectively. Indeed, the baseline average seasonal cumulative rainfall of Cesa was only 194 mm which was not sufficient to meet the CWR of soybean (Gajić et al., 2018; Rittler and Bykova, 2022). Except for Ljubljana, our results were higher than recent global WF assessments (2010–2019) for soybean under rainfed (1549 m^3 ton^{-1}) and irrigated (1601 m^3 ton^{-1}) conditions (Mialyk et al., 2024). Our findings were aligned with the estimates of Mekonnen and Hoekstra (2011), suggesting that as yield decreases, the WF tends to increase. Based on the baseline climatic data, our results emphasized that no significant increase in soybean WF across irrigation strategies could have been observed if irrigation was implemented in the period between 1981–2010. This may have been due to yield stability effects as a result of irrigation buffering the impacts of climate fluctuations (Barrera et al., 2024).

Soybean, having been cultivated under rainfed conditions in the past across study sites, relied primarily on green WF, corroborating the results of other studies (Ding et al., 2019; Zhao et al., 2022). The green WF in Castelfranco and Cesa were higher than the current global green WF for soybean (1549 m^3 ton^{-1}) from 2010 to 2019. In the same time period, Mialyk et al. (2024) reported green WF values of 1104 m^3 ton^{-1} for Italy and 1669 m^3 ton^{-1} for Slovenia. The present results in Castelfranco and Ljubljana were close to these assessments whereas, the result in Cesa was relatively higher. The overall findings confirmed that the rainfall pattern in the past could have directly impacted the green WF of soybean, showing a negative correlation. Interestingly, yield has emerged as the primary driver of WF variations (Wang et al., 2023; Zhao et al., 2022).

In this study, the blue water was assumed to be exclusively derived from irrigation, even though capillary rise has been reported as an alternative source (Chukalla et al., 2015). The simulations showed significant variation in blue water across different irrigation strategies in Castelfranco and Cesa, with the exception between 25% and 50% RAW depletion. However, in Ljubljana, blue water was only affected when RAW was completely depleted. These results suggested that the effects of irrigation became apparent when seasonal rainfall declined significantly below the threshold (300 mm) required for soybean cultivation (Gajić et al., 2018), as was observed in Castelfranco and Cesa. Thus, Ljubljana, with the highest rainfall and lowest net irrigation, also registered the lowest blue water. Instead, the opposite was true for Cesa.

Across irrigation strategies, simulations showed that by maintaining 100% RAW depletion as the threshold to start the irrigation, there was a resultant adverse impact on grain yield. This was particularly evident in Cesa, which also had the lowest blue water. These combined effects explained why the lowest blue WF was observed at this threshold. Conversely, the highest blue WF in all locations was observed at 25% RAW depletion due to the elevated blue water content. Although we only evaluated one irrigation strategy below 50% RAW depletion, the simulations suggest that below this threshold, irrigation would become less efficient. These findings demonstrated that the 50% RAW depletion could have been a viable irrigation strategy to reduce blue WF without significantly negatively affecting soybean grain yield had it been implemented between 1981 to 2010. Our results were lower

than the average blue WF (926 m^3 ton^{-1}) of irrigated soybean for the period 1996–2005 (Mekonnen and Hoekstra, 2011). This variation is primarily attributed to the predominant rainfed cultivation of soybean worldwide which entails no use of irrigation and, therefore, zero blue WF. Nevertheless, the simulations indicated that a higher blue WF and a greater irrigation volume were needed for soybean production in Cesa compared to Castelfranco and Ljubljana.

4.2 Water footprints and water use under climate change scenarios

4.2.1 Impacts of climate change under rainfed conditions

The simulations showed variable impacts of climate change on $WF_{rainfed}$ across locations. In Castelfranco and Cesa, climate change generally reduced the $WF_{rainfed}$ as indicated by lower values across SSPs compared to the baseline. Furthermore, in Castelfranco, the slight increase in $WF_{rainfed}$ in the far future under SSP1-2.6 compared to the baseline may be attributed to a reduction in yield. The yield reduction was a consequence of decreased CO_2 fertilization effects due to the combination of increased temperature and the absence of irrigation water. Consequently, in Ljubljana, climate change increased the $WF_{rainfed}$ in all time periods. The exceptions were for SSP2-4.5 and for SSP1-2.6 in the mid-future in which a slight decrease was observed. This signified that even the less detrimental increase in temperature in these two emissions scenarios, coupled with elevated CO_2 levels, could facilitate a change in WF. The dynamics of $WF_{rainfed}$ across locations may also be explained by the combined effects of reduced grain yield and CWR (Supplementary Tables 4, 5), resulting from a shortened growing period. This shorter cycle was due to the faster accumulation of GDD as a consequence of increased temperature, which in turn, reduced the time available for biomass accumulation and yield formation.

Across locations, the $WF_{rainfed}$ dynamics of each SSP varied across time periods. However, in general, $WF_{rainfed}$ increased from the mid to far future under SSP1-2.6 and SSP5-8.5 and decreased under SSP2-4.5 from the near to far future. Wang et al. (2023) mentioned that rainfall and temperature are two of the main climatic factors influencing WF in crop production. Thus, the increased temperature and reduced rainfall under SSP5-8.5 (Supplementary Table 1) negatively affected soybean performance by increasing WF. The overall results followed the opposite trend of grain yield, indicating that the soybean WF dynamics in the future will be primarily associated with future changes in crop yield (Arunrat et al., 2022; Mekonnen and Hoekstra, 2011).

Rainfall is the only source of green water under rainfed conditions. The green water was highest in Ljubljana and lowest in Cesa. Thus, these results were expected given the abundant and scarce rainfall in Ljubljana and Cesa, respectively (Supplementary Table 1). In all locations, the green water was higher in the baseline period compared to the SSPs, indicating that climate change reduced green water. This may be attributed to the reduced rainfall and shortened growing cycle due to the accelerated accumulation of GDD resulting from increased temperature.

4.2.2 Impacts of climate change under irrigated conditions

Irrigating soybean would require additional WFs, thus the $WF_{irrigated}$ was foreseen to be higher than $WF_{rainfed}$ due to the addition of blue WF from irrigation. The impact of climate change on $WF_{irrigated}$ varied across locations. In Castelfranco and Cesa, irrigation acted as a buffer against the negative effects of climate change and maximized CO_2 fertilization effects that ultimately resulted in a slight yield increase. This was further supported by our results in rainfed conditions, indicating that despite increased CO_2 levels, low yield under SSPs compared to the baseline was observed due to lack of irrigation (Supplementary Tables 1, 4). This result confirmed previous work showing that CO_2 fertilizing effects can only be realized if soybean is irrigated (Ainsworth and Long, 2021). The CWR decreased both under rainfed and irrigated conditions (Supplementary Table 5), which confirmed that temperature was the main driving factor for the change. Thus, the reduction in $WF_{irrigated}$ in Castelfranco and Cesa under climate change scenarios was attributed to a slight increase in grain yield due to irrigation and CO_2 fertilization, as well as a decrease in CWR. The reduction in CWR resulted from a shortened growing cycle, driven by faster GDD accumulation caused by both rising temperatures and the CO_2 fertilization effect, which also reduces crop transpiration (Raes, 2023). Consequently, no increase in grain yield under climate change scenarios was observed in Ljubljana due to a reduced buffering effect of irrigation as a result of the abundant projected rainfall in the area. However, reduced CWR was still observed due to increased temperature (Supplementary Tables 1, 5). On one hand, when rainfall is abundant, the benefits of irrigation are reduced and the negative impact of climate change intensifies leading to an increased WF. On the other hand, when rainfall is reduced, the benefits of irrigation are maximized by increasing grain yield which is further enhanced by CO_2 fertilization effects, ultimately leading to a decreased WF. Nevertheless, the overall results conformed to the expectation that both temperature and rainfall will facilitate future changes in the WF of crops (Wang et al., 2023).

Considering the dynamics of $WF_{irrigated}$ among SSPs across time periods, as was expected, an increase was confirmed in all locations under the most pessimistic scenario (SSP5-8.5). In addition, the reduced CO_2 concentration from the mid to far future under SSP1-2.6 also led to an increased WF. Instead, following the intermediate path (SSP2-4.5), the $WF_{irrigated}$ decreased in all locations from the near to far future. These results further confirmed the influence of CO_2 fertilization and increased temperature on WF, as discussed previously.

In all locations, the blue water was higher across SSPs compared to the baseline, indicating negative impacts of climate change and confirming the expectation that climate change will increase both the evaporative demand and blue WF of crops in the future (Arunrat et al., 2022; Toreti et al., 2022; Wang et al., 2023). The results corroborated the NIR results, where the same pattern was observed across locations (Supplementary Table 6). In our simulations, given that irrigation was the only source of blue water, these results were anticipated. Thus, blue water is projected to increase in the future. This signifies that more

irrigation volume will be needed to produce soybean with values exceeding those in Cesa, compared to Castelfranco and Ljubljana, due to reduced rainfall.

Considering irrigation strategies, a general pattern of decreased blue WF was observed as the percentage of RAW depletion to start irrigation increased. The result was a consequent reduction in grain yield. This is explained by the direct relationship of blue WF with blue water and NIR. Our results highlighted that trade-offs like yield reduction need to be considered when implementing irrigation strategies to reduce WFs of soybean production. Nevertheless, the results indicated that in all locations, 50% RAW depletion in the ERZ should be maintained to reduce the blue WF without a significant reduction in soybean grain yield.

4.3 Relative changes in yield and consumptive water footprints

In all locations, the highest yield reduction occurred under rainfed conditions, especially in the mid and far future scenarios under SSP5-8.5. This result clearly highlighted the vulnerability of rainfed soybean cultivation to climate change. The overall impact of irrigation was assessed by calculating the relative change in soybean performance of each irrigation strategy with the rainfed conditions. Under irrigated conditions, positive changes in yield were observed in all locations which indicated that irrigation can act as a buffer against the negative effects of climate change, to maintain or increase soybean grain yield. Thus, irrigation represents a viable adaptation strategy to increase soybean productivity. The findings suggested that irrigating soybean in Castelfranco and Cesa would offer greater benefits, whereas the incremental yield due to irrigation in Ljubljana would be marginal due to relatively abundant rainfall in the area. The results further showed that the soybean consumptive WFs could be reduced by allowing a greater depletion of RAW in the root zone before starting irrigation. This approach would also decrease the NIR, which in turn would reduce both the blue water and blue WF. Among irrigation strategies, although the 100% RAW depletion showed the highest reduction in consumptive WFs, the 50% RAW depletion can be seen to offer an advantage by not significantly affecting the grain yield. While the relative increase in yield and reduction in consumptive WFs were slightly higher under SSP2-4.5, the findings underscore that the trend of climate change impacts on soybean under irrigated conditions were generally consistent across irrigation strategies, varying only slightly in intensity based on location, SSPs, and time periods.

The overall impact of climate change was assessed by calculating the relative change in soybean performance of each SSP with the baseline. In Ljubljana, the simulations showed that soybean yield declined more sharply under rainfed conditions compared to irrigated conditions. Although irrigation helped mitigate the impacts of climate change on soybean yield, this benefit did not extend to the SSP5-8.5 scenario projected for the distant future. Ultimately, irrigation can merely sustain soybean yield. This indicates that the impact of climate change will be more detrimental when rainfall is abundant and with slightly lower T_{min} and T_{max}. Consequently, the simulated grain yield in Castelfranco and Cesa was generally increased under SSP2-4.5 which indicates that the less detrimental increase of temperature (2.2–4.2°C) in this emission scenario is currently being offset by irrigation and increased CO_2 levels (Araji et al., 2018; Durodola and Mourad, 2020; Sharafati et al., 2022). In the near and mid future, despite an increase in yield under SSP5-8.5 in Castelfranco and Cesa, a decline in grain yield in the far future was predicted across locations except in Castelfranco. This confirmed that the fertilizing effects of CO_2 cannot be guaranteed at such high increase in temperature (2.9–7.8°C), posing detrimental impacts on soybean performance (Lin et al., 2021; Schauberger et al., 2017). Minimal increases in grain yield were also observed in Castelfranco and Cesa under SSP1-2.6, even though the temperature increase was the least (1.8–3.1°C). This indicated that the CO_2 fertilization effects are also minimal when CO_2 level is low. In all locations, climate change is expected to reduce the CWR of soybean. In the real world, crops close their stomata in response to increased temperature. As a consequence, transpiration is reduced which also reduces CWR and eventually decreases yield. To compensate for the yield losses, NIR is, therefore, required to increase. Overall, these changes in CWR and NIR were shown to have direct influences on consumptive WFs, as was observed in the study sites. In Ljubljana, climate change increased the consumptive WFs as a consequence of reduction in yield and CWR. In contrast, the decreased consumptive WFs in Castelfranco and Cesa can be attributed to reduced CWR alongside slight increase in yield.

5 Conclusions

The impacts of climate change on the WFs of soybean in central (Cesa) and north (Castelfranco) Italy and in central Slovenia (Ljubljana) were investigated in this study using baseline and future climate scenarios. Simulations showed that from 1981 to 2010, soybean production in the three locations was primarily dependent on green WF. $WF_{rainfed}$ was predominantly influenced by crop yield and CWR, in turn affected by rainfall and temperature variations. Irrigation increased the soybean grain yield and blue WF, particularly when RAW depletion to start irrigation was reduced. $WF_{irrigated}$ remained relatively stable across different irrigation strategies. Considering future climate scenarios across time periods, a decline in green water is anticipated alongside increases in blue water and blue WF under SSP5-8.5. Moreover, both $WF_{rainfed}$ and $WF_{irrigated}$ are projected to increase in the near to far future under SSP5-8.5 but to decrease under SSP2-4.5. These findings underscore the suitability of Ljubljana for soybean cultivation, but at the same time highlight the greater vulnerability to climate change compared with Castelfranco and Cesa. Soybean irrigation in Castelfranco and Cesa is highly recommended to maximize yield. However, despite irrigation, the yield potential in Cesa will remain marginal due to increased temperature and reduced rainfall. Instead, the yield increase due to irrigation in Ljubljana will remain minimal due to abundant rainfall. The irrigation strategies affected yield, blue water, and blue WF more significantly than the consumptive WFs. These results highlighted that trade-offs between decreasing yield and increasing blue WF need to be considered when implementing irrigation strategies across the study sites. While optimal levels of RAW depletion vary by location, a

50% depletion could be a viable irrigation strategy, effectively reducing WFs without significantly compromising soybean grain yield. The results of this study are subject to model uncertainty and input limitations, emission scenario dependency, and the limited scope of irrigation strategies and other field management practices. Socioeconomic factors, regional specificity, and potential constraints on future irrigation availability could also affect the applicability and accuracy of the findings. Despite these uncertainties, the study offers important insights into how climate change affects soybean WFs, emphasizing the growing dependence on blue water in future scenarios. The findings are crucial for making informed decisions to support sustainable soybean production in the study areas. While these results provide crucial insights, the study is subject to model uncertainty and dependence on emission scenarios. Furthermore, it does not account for the grey water footprint or the socioeconomic factors that may influence future production. Future research should therefore integrate a broader range of field management practices and analyze potential constraints on water availability to refine climate change adaptation strategies for soybean.

Data availability statement

The original contributions presented in the study are included in the article/Supplementary Material. Further inquiries can be directed to the corresponding author.

Author contributions

WB: Formal analysis, Investigation, Methodology, Writing – original draft. FM: Methodology, Writing – original draft. CM: Methodology, Supervision, Writing – review & editing. MG: Conceptualization, Validation, Writing – review & editing. TP: Methodology, Supervision, Writing – review & editing. MF: Methodology, Writing – review & editing. GG: Conceptualization, Supervision, Writing – review & editing. LV: Investigation, Visualization, Writing – review & editing. RF: Methodology, Supervision, Writing – review & editing. AD: Conceptualization, Supervision, Writing – review & editing.

Funding

The author(s) declared that financial support was received for this work and/or its publication. This study was funded by the PRIN 2020 project "Looking back to go forward: reassessing crop water requirements in the face of global warming" (REWATERING) funded by the Italian Ministry of University and Research (CUP: B53C22000110006; code: 2020FFWTJR_003). The research in Slovenia was funded by the Slovenian Research Agency program under the grant agreement P4-0085.

Acknowledgments

The research in Italy was supported by the PRIN 2020 project "Looking back to go forward: reassessing crop water requirements in the face of global warming" (REWATERING) funded by the Italian Ministry of University and Research (CUP: B53C22000110006; code: 2020FFWTJR_003). The simulation experiments for Ljubljana were conducted by the first author during his research period abroad at the University of Ljubljana as part of a PhD program in Sustainable Development and Climate Change.

Conflict of interest

The author(s) declared that this work was conducted in the absence of any commercial or financial relationships that could be construed as a potential conflict of interest.

Correction note

A correction has been made to this article. Details can be found at: 10.3389/fagro.2026.1808128.

Generative AI statement

The author(s) declared that generative AI was not used in the creation of this manuscript.

Any alternative text (alt text) provided alongside figures in this article has been generated by Frontiers with the support of artificial intelligence and reasonable efforts have been made to ensure accuracy, including review by the authors wherever possible. If you identify any issues, please contact us.

Publisher's note

Supplementary material

The Supplementary Material for this article can be found online at: https://www.frontiersin.org/articles/10.3389/fagro.2026.1748798/full#supplementary-material

References

Ainsworth, E. A., and Long, S. P. (2021). 30 years of Free-Air Carbon Dioxide Enrichment (FACE): what have we learned about future crop productivity and the potential for adaptation? *Global Change Biol.* 27, 27–49. doi: 10.1111/gcb.15375

Allen, R. G., Pereira, L. S., Raes, D., and Smith, M. (1998). *Crop Evapotranspiration-Guidelines for Computing Crop Water Requirements-FAO Irrigation and Drainage Paper 56* (Rome, Italy: FAO).

Araji, H. A., Wayayok, A., Bavanic, A. M., Amirid, E., Abdullaha, A. F., Daneshiane, J., et al. (2018). Impacts of climate change on soybean production under different treatments of field experiments considering the uncertainty of general circulation Models. *Agric. Water Manage.* 205, 63–71. doi: 10.1016/j.agwat.2018.04.023

Arunrat, N., Sereenonchai, S., Chaowiwat, W., and Wang, C. (2022). Climate change impact on major crop yield and water footprint under CMIP6 climate projections in repeated drought and flood areas in Thailand. *Sci. Total Environ.* 807, 150741. doi: 10.1016/j.scitotenv.2021.150741

Ayala, L. M., Eupen, M., Zhang, G., Pérez-Soba, M., Martorano, L. G., Lisboa, L. S., et al. (2016). Impact of agricultural expansion on water footprint in the Amazon under climate change scenarios. *Sci. Total Environ.* 569–570, 1159–1173. doi: 10.1016/j.scitotenv.2016.06.191

Barrera, W., Morbidini, F., Zammarchi, L., Ghinassi, G., Maucieri, C., Borin, M., et al. (2024). Assessing the impacts of regulated deficit irrigation on soybean using AquaCrop. *Ital. J. Agron.* 19, 100023. doi: 10.1016/j.ijagro.2024.100023

Bocchiola, D., Nana, E., and Soncini, A. (2013). Impact of climate change scenarios on crop yield and water footprint of maize in the Po valley of Italy. *Agric. Water Manage.* 116, 50–61. doi: 10.1016/j.agwat.2012.10.009

Chapagain, A. K., Hoekstra, A. Y., Savenije, H. H. G., and Gautam, R. (2006). The water footprint of cotton consumption: an assessment of the impact of worldwide consumption of cotton products on the water resources in the cotton producing countries. *Ecol. Econ.* 60, 186–203. doi: 10.1016/j.ecolecon.2005.11.027

Chukalla, A. D., Krol, M. S., and Hoekstra, A. Y. (2015). Green and blue water footprint reduction in irrigated agriculture: effect of irrigation techniques, irrigation strategies and mulching. *Hydrol. Earth Syst. Sci.* 19, 4877–4891. doi: 10.5194/hess-19-4877-2015

Ding, X., Wang, S., and Chen, B. (2019). The blue, green and grey water consumption for crop production in Heilongjiang. *Energy Proc.* 158, 3908–3914. doi: 10.1016/j.egypro.2019.01.853

Durodola, O. S., and Mourad, K. A. (2020). Modeling the impacts of climate change on soybeans water use and yields in Ogun-Ona River. *Agriculture* 10, 593. doi: 10.3390/agriculture10120593

European Parliament (2023) *European Parliament Resolution on a European Protein Strategy, Publications Office of the European Union* (Belgium). (2023/2015(INI)).

Falkenmark, M., and Rockström, J. (2006). The new blue and green water paradigm: Breaking new ground for water resources planning and management, J. Water Resour. *Plann. Manage.* 3, 129–132. doi: 10.1061/(ASCE)0733-9496(2006)132:3(129)

Flach, R., Skalský, R., Folberth, C., Balkovič, J., Jantk, K., and Schneider, U. A. (2020). Water productivity and footprint of major Brazilian rainfed crops – A spatially explicit analysis of crop management scenarios. *Agric. Water Manage.* 233, 105996. doi: 10.1016/j.agwat.2019.105996

Flajšman, M., Šantavec, I., Kolmanič, A., and Ačko, D. K. (2019). Bacterial seed inoculation and row spacing affect the nutritional composition and agronomic performance of soybean. *Int. J. Plant Production* 13, 183–192. doi: 10.1007/s42106-019-00046-8

Food and Agriculture Organization Statistics (FAOSTAT) (2024). Available online at: https://www.fao.org/faostat/en/#data/QCL (Accessed April 03, 2024).

Gajić, B., Kresović, B., Tapanarova, A., Životića, L., and Todorović, M. (2018). Effect of irrigation regime on yield, harvest index and water productivity of soybean grown under different precipitation conditions in a temperate environment. *Agric. Water Manage.* 210, 224–231. doi: 10.1016/j.agwat.2018.08.002

Gao, J., Zhuo, L., Duan, X., and Wu, P. (2023). Agricultural water-saving potentials with water footprint bench marking under different tillage practices for crop production in an irrigation district. *Agric. Water Manage.* 282, 108274. doi: 10.1016/j.agwat.2023.108274

Hiel, R., Geling, V., de Vries, T., Lan, C., and Sleurink, N. (2018). *European soy Monitor-Insights on European Responsible and Deforestation-Free Soy Consumption in 2018.* (Rome: The Sustainable Trade Initiative).

Hoekstra, A. Y. (2017). Water footprint assessment: evolvement of a new research field. *Water Resour. Manage.* 31, 3061–3081. doi: 10.1007/s11269-017-1618-5

Hoekstra, A. Y., and Chapagain, A. K. (2007). Water footprints of nations: water use by people as a function of their consumption pattern. *Water Resour. Manage.* 21, 35–48. doi: 10.1007/s11269-006-9039-x

Hoekstra, A. Y., Chapagain, A. K., Aldaya, M. M., and Mekonnen, M. M. (2011). *The Water Footprint Assessment Manual: Setting the Global Standard* (London, UK: Earthscan).

Hoekstra, A. Y., and Hung, P. Q. (2002). *Virtual water trade: a quantification of virtual water flows between nations in relation to international crop trade* (Delft, The Netherlands: UNESCO-IHE), 12–13.

Jiang, T., Sun, S., Li, Z., Li, Q., Lu, Y., Li, C., et al. (2022). Vulnerability of crop water footprint in rain-fed and irrigation agricultural production system under future climate scenarios. *Agric. For. Meteorology* 326, 109164. doi: 10.1016/j.agrformet.2022.109164

Lawless, C., and Semenov, M. A. (2005). Assessing lead-time for predicting wheat growth using a crop simulation model. *Agric. For. Meteorol.* 135 (1-4), 302–313. doi: 10.1016/j.agrformet.2006.01.002

Li, Z., Feng, B., Wang, W., Yang, X., Wu, P., and Zhuo, L. (2022). Spatial and temporal sensitivity of water footprint assessment in crop production to modeling inputs and parameters. *Agric. Water Manage.* 271, 107805. doi: 10.1016/j.agwat.2022.107805

Lin, T.-S., Song, Y., Lawrence, P., Kheshgi, H. S., and Jain, A. K. (2021). Worldwide maize and soybean yield response to environmental and management factors over the 20th and 21st centuries. *J. Geophysical Research: Biogeosciences* 126, e2021JG006304. doi: 10.1029/2021JG006304

Meinshausen, M., Vogel, E., Nauels, A., Lorbacher, K., Meinshausen, N., Etheridge, D. M., et al. (2017). Historical greenhouse gas concentrations for climate modeling (CMIP6). *Geosci. Model. Dev.* 10, 2057–2116. doi: 10.5194/gmd-10-2057-2017

Meinshausen, M., Nicholls, Z. R.., Lewis, J., Gidden, M. J., Vogel, E., Freund, M., et al. (2020). The shared socio-economic pathway (SSP) greenhouse gas concentrations and their extensions to 2500. *Geoscientific Model. Dev.* 13, 3571–3605. doi: 10.5194/gmd-13-3571-2020

Mekonnen, M. M., and Hoekstra, A. Y. (2011). The green, blue and grey water footprint of crops and derived crop products. *Hydrol. Earth Syst. Sci.* 15, 1577–1600. doi: 10.5194/hess-15-1577-2011

Mekonnen, M. M., and Hoekstra, A. Y. (2014). Water footprint benchmarks for crop production: a first global assessment. *Ecol. Indic.* 46, 214–223. doi: 10.1016/j.ecolind.2014.06.013

Mialyk, O., Schyns, J. F., Booij, M. J., Su, H., Hogeboom, R. J., and Berger, M. (2024). Water footprints and crop water use of 175 individual crops for 1990–2019 simulated with a global crop model. *Sci. Data* 11, 206. doi: 10.1038/s41597-024-03051-3

Nendel, C., Reckling, M., Debaeke, P., Schulz, S., Berg-Mohnicke, M., Constantin, J., et al. (2023). Future area expansion outweighs increasing drought risk for soybean in Europe. *Glob Change Biol.* 29, 1340–1358. doi: 10.1111/gcb.16562

Pereira, L. S., Allen, R. G., Smith, M., and Raes, D. (2015). Crop evapotranspiration estimation with FAO56: Past and future. *Agric. Water Manage.* 147, 4–20. doi: 10.1016/j.agwat.2014.07.031

Pereira, L. S., and Alves, I. (2013). "Crop water requirements." in *Encyclopedia of Soils in the Environment.* (Elsevier Inc.). doi: 10.1016/B978-0-12-409548-9.05129-0

Raes, D., Steduto, P., Hsiao, T. C., and Fereres, E. (2022). "Chapter 2: users guide," in *AquaCrop version 7.0. Reference Manual* (Food Agricultural Organization (FAO, Rome, Italy), 2–372.

Raes, D. (2023). *AquaCrop training handbook I. Understanding AquaCrop* (Rome, Italy: Food Agricultural Organization (FAO), 2–372.

R Core Team (2021). *R: A language and environment for statistical computing* (Vienna, Austria: R Foundation for Statistical Computing). Available online at: https://www.R-project.org/.

Rittler, L., and Bykova, O. (2022). Water use and irrigation in soybean. *Legume Translated*, 221-255.

Rodriguez, P. O., Holzman, M. E., Aldaya, M. M., and Rivas, R. E. (2024). Water footprint in rainfed summer and winter crops: The role of soil moisture. *Agric. Water Manage.* 296, 108787. doi: 10.1016/j.agwat.2024.108787

Rodriguez, P. O., Holzmana, M. E., Deganob, M. F., Faramiñán, A. M. G., Rivas, R. E., and Bayala, M. I. (2021). Spatial variability of the green water footprint using a medium-resolution remote sensing technique: The case of soybean production in the Southeast Argentine Pampas. *Sci. Total Environ.* 763, 142963. doi: 10.1016/j.scitotenv.2020.142963

Santos, J. F. S., and Naval, L. P. (2020). Spatial and temporal dynamics of water footprint for soybean production in areas of recent agricultural expansion of the Brazilian savannah (Cerrado). *J. Cleaner Production* 251, 119482. doi: 10.1016/j.jclepro.2019.119482

Santos, J. F. S., and Naval, L. P. (2022). Soy water footprint and socioeconomic development: An analysis in the new agricultural expansion areas of the Brazilian cerrado (Brazilian savanna). *Environ. Dev.* 42, 100670. doi: 10.1016/j.envdev.2021.100670

Schauberger, B., Archontoulis, S., Arneth, A., Balkovic, J., Ciais, P., Deryng, D., et al. (2017). Consistent negative response of US crops to high temperatures in observations and crop models. *Nat. Commun.* 8, 13931. doi: 10.1038/ncomms13931

Semenov, M. A., Barrow, E. M., and Lars-Wg, A. (2002). *A stochastic weather generator for use in climate impact studies.*. (User Man Herts UK), 1–27.

Shang, K., Zhuo, L., Yang, X., Yue, Z., Zhao, D., and Wu, P. (2021). Emergy analysis of the blue and green water resources in crop production systems. *J. Cleaner Production* 319, 128666. doi: 10.1016/j.jclepro.2021.128666

Sharafati, A., Tayyebi, M. M., Pezeshki, E., and Shahid, S. (2022). Uncertainty of climate change impact on crop characteristics: a case study of Moghan plain in Iran. *Theor. Appl. Climatology* 149, 603–620. doi: 10.1007/s00704-022-04074-9

Steduto, P., Hsiao, T. C., Raes, D., and Fereres, E. (2009). AquaCrop-the FAO crop model to simulate yield response to water: I. Concepts and underlying principles. *Agron. J.* 101, 426–437. doi: 10.2134/agronj2008.0139s

Toreti, A., Bavera, D., Acosta Navarro, J., Cammalleri, C., de Jager, A., Di Ciollo, C., et al. (2022). *Drought in Europe August 2022* (Luxembourg: Publications Office of the European Union), JRC130493. doi: 10.2760/264241

Vanuytrecht, E., Raes, D., Steduto, P., Hsiao, T. C., Fereres, E., Heng, L. K., et al. (2014). AquaCrop: FAO's crop water productivity and yield response model. *Environ. Modeling Software* 62, 351e360. doi: 10.1016/j.envsoft.2014.08.005

Ventrella, D., Giglio, L., Garofalo, P., and Dalla Marta, A. (2017). Regional assessment of green and blue water consumption for tomato cultivated in Southern Italy. *J. Agric. Sci*. 156, 689–01. doi: 10.1017/S0021859617000831

Wang, Q., Huang, K., Liu, H., and Yu, Y. (2023). Factors affecting crop production water footprint: A review and meta-analysis. *Sustain. Production Consumption* 36, 207–216. doi: 10.1016/j.spc.2023.01.008

Xu, Y., Huang, K., Yu, Y., and Wang, X. (2015). Changes in water footprint of crop production in Beijing from 1978 to 2012: a logarithmic mean Divisia index decomposition analysis. *J. Clean. Prod.* 87, 180–187. doi: 10.1016/j.jclepro.2014.08.103

Yeşilköy, S., and Şaylan, L. (2020). Assessment and modeling of crop yield and water footprint of winter wheat by aquacrop. *Ital. J. Agrometeorology* 3), 3–14. doi: 10.13128/ijam-859

Zhao, J., Han, T., Wang, C., Shi, X., Wang, K., Zhao, M., et al. (2022). Assessing variation and driving factors of the county-scale water footprint for soybean production in China. *Agric. Water Manage.* 263, 107469. doi: 10.1016/j.agwat.2022.107469

Zhuo, L., Mekonnen, M. M., and Hoekstra, A. Y. (2016a). The effect of inter-annual variability of consumption, production, trade and climate on crop-related green and blue water footprints and inter-regional virtual water trade: A study for China, (1978-2008). *Water Res.* 94, 73e85. doi: 10.1016/j.watres.2016.02.037

Zhuo, L., Mekonnen, M. M., and Hoekstra, A. Y. (2016c). Consumptive water footprint and virtual water trade scenarios for China—With a focus on crop production, consumption and trade. *Environ. Int.* 94, 211–223. doi: 10.1016/j.envint.2016.05.019

Zhuo, L., Mekonnen, M. M., Hoekstra, A. Y., and Wada, Y. (2016b). Inter-and intra-annual variation of water footprint of crops and blue water scarcity in the yellow river basin, (1961-2009). *Adv. Water Resour.* 87, 29–41. doi: 10.1016/j.advwatres.2015.11.002